How robust is the hydrogen-bonded amide 'ladder' motif?†

Christer B. Aakeröy,* Benjamin M. T. Scott and John Desper

Received (in Montpellier, France) 11th October 2007, Accepted 29th October 2007
First published as an Advance Article on the web 6th November 2007
DOI: 10.1039/b715610c

The well-known hydrogen-bonded ladder displayed by amides in the solid state, is readily disrupted and reduced to an $R_2^2(8)$ motif if a competitive hydrogen-bond acceptor is incorporated in the molecular structure of the amide. When a weaker hydrogen-bond acceptor (*i.e.* $-NO_2$, –CN, –Cl, –Br) is present, the ladder persists in about every other case, whereas if a stronger hydrogen-bond acceptor is introduced (such as a N-heterocycle), the ladder is very unlikely to appear. If a strong hydrogen-bond acceptor is present, the amide···amide dimer 'survives' a little over 50% of the time. This conclusion is based upon the synthesis and structural characterization of six pyrazole-decorated benzamides in addition to an examination of relevant data from the CSD. The *anti* hydrogen atom of the amide moiety is much more likely to engage in an N–H···N(heterocycle) hydrogen bond instead of an N–H···O=C (amide) interaction.

Introduction

The way in which discrete molecules equipped with a variety of functional groups interact, bind and communicate with each other through non-covalent intermolecular forces[1] is central to our understanding of biological chemistry as well as to many areas of materials science (pharmaceutical compounds,[2] polymers,[3] liquid crystals,[4] organogelators,[5] and lithographic plates,[6]). On a fundamental level it is important to be able to identify patterns of behavior of functional groups but not just in terms of their chemical reactivity. We also need to acquire an improved understanding of non-covalent interactions in order to reliably predict molecular organization, assembly, and connectivity in the solid state as this ultimately controls many physical properties of the bulk materials.[7] In this context, single-crystal structural data have offered invaluable information regarding recurring intermolecular motifs, supramolecular synthons,[8] and interactions involving specific chemical functional groups, with the concept of synthons becoming key to advancing all practical manifestations of crystal engineering.[9]

The structural chemistry of the amide moiety has received considerable attention partly due to the self-complementary nature of its hydrogen-bond donors/acceptors, but also because of the abundance of amide moieties in biological systems.[10] The amide is, on its own, frequently associated with an infinite ladder-like motif typically composed of two pairs of symmetry related N–H···O hydrogen bonds.[11] The ladder is the result of a self-complementary, $R_2^2(8)$ homomeric amide···amide dimer Scheme 1(a) accompanied by N–H···O interactions between the *anti* hydrogen atom of the $-NH_2$ group and the carbonyl oxygen of an adjacent amide moiety (producing an $R_4^2(8)$ motif). This intermolecular arrangement satisfies both hydrogen-bond donors (the $-NH_2$ hydrogen atoms) and the two hydrogen-bond acceptor sites (the lone-pairs) on the carbonyl oxygen atom, Scheme 1(b).

Complications may arise, however, if additional hydrogen-bond acceptors are present on the same molecule as the amide. For example, in one of the polymorphs of 4-nitrobenzamide, the $-NO_2$ moiety disrupts the ladder-motif by acting as a hydrogen-bond acceptor for the $-NH_2$ *anti* hydrogen atom of the amide.[12]

In order to address this challenge, we have carried out a systematic structural study of a family of new compounds comprising an amide moiety and an N-heterocyclic fragment, Scheme 2. The relative basicity, and thus ability to form hydrogen bonds, of the N-heterocycle can be varied through simple covalent modifications, which offers a practical tool for establishing reliable correlations between molecular structure/function and supramolecular assembly/organization.

We have also supplemented the new structural information with relevant data obtained from the CSD.[13] The literature search was confined to (a) compounds containing a benzamide-type fragment accompanied by an additional functional group capable of acting as a hydrogen-bond acceptor only (such as $-NO_2$, –OMe –CN, –Cl, –Br), and (b) compounds

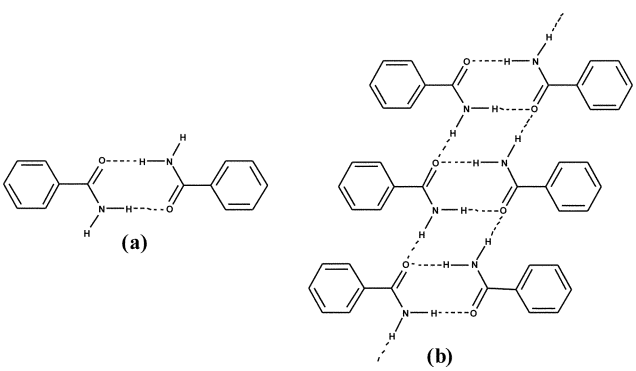

Scheme 1 (a) Homomeric amide dimer; (b) extended ladder.

Department of Chemistry, Kansas State University, 111 Willard Hall, Manhattan, KS, USA. E-mail: aakeroy@ksu.edu; Fax: 785 532 6666; Tel: 785 532 6665

† Electronic supplementary information (ESI) available: X-Ray experimental details. See DOI: 10.1039/b715610c

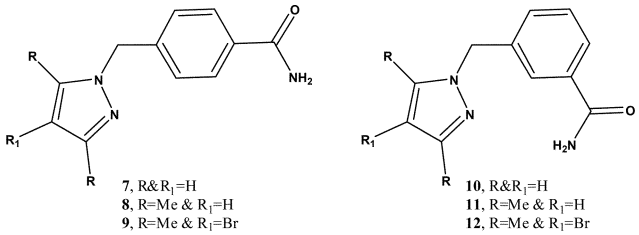

Scheme 2 Pyrazole based benzamides.

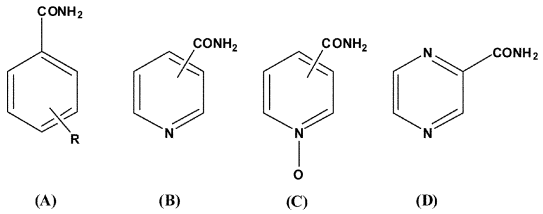

Scheme 3 CSD search parameters (A: substituted benzamides, B: isonicotinamide and nicotinamide, C: *N*-oxide of isonicotinamide and nicotinamide, D: pyrazine amide).

comprising a N-heterocyclic fragment substituted with an amide moiety, Scheme 3.

The combination of our new structural data with relevant information from the CSD produces a sufficiently large number of structures to enable us to explicitly address three questions:

I. How reliable is the amide *ladder* in the organic solid state if competing hydrogen-bond sites are present?

II. How reliable is the amide···amide *dimer* in the presence of competing hydrogen-bond acceptors?

III. Is it possible to rank different functional groups according to how likely they are to disrupt the ladder by interacting with the amino *anti* hydrogen atom of the amide moiety?

Experimental

Synthesis

All chemicals were purchased from Aldrich and Fischer and used without further purification. 4-bromo-3,5-dimethylpyrazole was synthesised *via* a previously published procedure.[14] Melting points were determined on a Fisher–Johns melting point apparatus and are uncorrected.

4-[(Pyrazol-1-ylmethyl)]benzonitrile, 1. To a round bottom flask, pyrazole (1.5 g, 22.1 mmol) and THF (80 ml) were added. To this solution, NaOH pellets (8.82 g, 221 mmol) were added and the reaction was stirred at room temperature for 2 h. On completion of the stir, α-bromo-*p*-tolunitrile (4.32 g, 22.1 mmol) in THF (80 ml) was added and the reaction mixture stirred at room temperature overnight. On completion, water was added to dissolve any excess NaOH, the organic layer was separated off, dried over $MgSO_4$ and the solvent removed under vacuum to yield a white solid (3.358 g, 83.3%). Mp 71–73 °C. ^{1}H NMR (δ_H; 400 MHz, $CDCl_3$): 5.392 (s, 2H), 6.339 (t, J = 2.2 Hz, 1H), 7.234–7.254 (d, J = 8 Hz, 2H), 7.445 (s, 1H), 7.584 (s, 1H), 7.615–7.636 (d, J = 8.4 Hz, 2H); IR (KBr): 3111.60, 2939.23, 2223.20, 1619.89, 1500.55, 1447.51, 1387.85, 1275.14, 1076.24, 1036.46, 950.28, 824.31, 744.75.

4-[(Pyrazol-1-ylmethyl)]benzamide, 7. To a round bottom flask, 4-[(pyrazol-1-ylmethyl)]benzonitrile (2.858 g, 15.60 mmol) and 85% H_2SO_4 (12 ml) were added. The mixture was heated to 80 °C and stirred for 4 h. On completion, the solution was poured slowly over ice and the resulting brown solution was adjusted to basic pH using 5 M NaOH. The aqueous solution was washed with $CHCl_3$ and the organic extracts were separated, dried over $MgSO_4$ and reduced to a white solid (2.627 g, 83.7%). Colourless plates suitable for X-ray diffraction were obtained *via* slow evaporation of ethanol. Mp 135–137 °C. ^{1}H NMR (δ_H; 400 MHz, $CDCl_3$): 5.400 (s, 2H), 5.570 (s, 1H), 6.020 (s, 1H), 6.330 (t, J = 2 Hz, 1H), 7.260–7.280 (d, J = 8 Hz, 2H), 7.430–7.436 (d, J = 2.4 Hz, 1H), 7.586–7.590 (d, J = 1.6 Hz, 1H), 7.779–7.800 (d, J = 4.4 Hz, 2H); ^{13}C NMR (δ_C; 50 MHz, $CDCl_3$): 55.389, 106.294, 127.605, 127.900, 129.516, 132.991, 139.963, 141.351, 168.761; IR (KBr): 3370.17, 3171.27, 3018.78, 2925.97, 1659.67, 1407.73, 1301.66, 1142.54, 923.76, 758.01. MS: m/z 201.983.

4-[(3,5-Dimethylpyrazol-1-ylmethyl)]benzonitrile, 2. To a round bottom flask, 3,5-dimethylpyrazole (0.5 g, 5.2 mmol) and THF (25 ml) were added. To this solution, NaOH pellets (2.1 g, 52.0 mmol) were added and the reaction was stirred at room temperature for 2 h. On completion, α-bromo-*p*-tolunitrile (1.04 g, 5.2 mmol) in THF (25 ml) was added and the reaction mixture stirred at room temperature for 3 days. On completion, water was added to dissolve any excess NaOH, the organic layer was separated off, dried over $MgSO_4$ and the solvent removed under vacuum to yield a white solid (0.936 g, 85%). Mp 63–65 °C. ^{1}H NMR (δ_H; 400 MHz, $CDCl_3$): 2.242 (s, 3H), 2.251 (s, 3H), 5.260 (s, 2H), 5.888 (s, 1H), 7.114–7.135 (d, J = 8.4 Hz, 2H), 7.572–7.593 (d, J = 8.4 Hz, 2H); IR (KBr): 3052.63, 2909.25, 2233.29, 1603.41, 1557.33, 1306.40, 1029.87, 809.67, 768.71, 548.51.

4-[(3,5-Dimethylpyrazol-1-ylmethyl)]benzamide, 8. To a round bottom flask, 4-[(3,5-dimethylpyrazol-1-ylmethyl)]-benzonitrile (10.99 g, 52.1 mmol) and 85% H_2SO_4 (100 ml) were added. The mixture was heated to 80 °C and stirred for 4 h. On completion, the solution was poured slowly over ice and the resulting brown solution was adjusted to basic pH using 5 M NaOH. The aqueous solution was washed with $CHCl_3$ and the organic extracts were separated, dried over $MgSO_4$ and reduced to a white solid (5.994 g, 50%). Colourless plates suitable for X-ray diffraction were obtained *via* slow evaporation of ethanol. Mp 172–175 °C. ^{1}H NMR (δ_H; 400 MHz, $CDCl_3$): 2.247 (s, 3H), 2.259 (s, 3H), 5.241 (s, 2H), 5.872 (s, 1H), 6.139 (s, 2H), 7.076–7.097 (d, J = 8.4 Hz, 2H), 7.735–7.756 (d, J = 8.4 Hz, 2H); ^{13}C NMR (δ_C; 50 MHz, $CDCl_3$): 11.253, 13.590, 52.258, 106.069, 126.939, 128.062, 132.705, 139.707, 141.627, 148.098 169.424; IR (KBr): 3446.94, 1680.23, 1644.38, 1413.94, 1383.21, 1306.40, 1116.93. MS: m/z 230.022.

4-[(4-Bromo-3,5-dimethylpyrazol-1-ylmethyl)]benzonitrile, 3. To a round bottom flask, 4-bromo-3,5-dimethylpyrazole (0.5 g, 2.86 mmol) and THF (25 ml) were added. To this

solution, NaOH pellets (1.14 g, 28.6 mmol) were added and the reaction was stirred at room temperature for 2 h. On completion, α-bromo-*p*-tolunitrile (0.56 g, 2.86 mmol) in THF (25 ml) was added and the reaction mixture stirred at room temperature for 2 days. On completion, water was added to dissolve any excess NaOH, the organic layer was separated off, dried over $MgSO_4$ and the solvent removed under vacuum to yield a white solid (2.082 g, 81.5%). Mp 76–79 °C. ^{1}H NMR (δ_H; 400 MHz, $CDCl_3$): 2.174 (s, 3H), 2.266 (s, 3H), 5.334 (s, 2H), 7.165–7.206 (d, J = 16.4 Hz, 2H), 7.603–7.645 (d, J = 16.8 Hz, 2H); IR (KBr): 3067.99, 2919.49, 2238.41, 1603.41, 1547.08, 1511.24, 1465.15, 1413.94, 1347.37, 1280.80, 1214.22, 1055.48, 809.67, 543.39.

4-[(4-Bromo-3,5-dimethylpyrazol-1-ylmethyl)]benzamide, 9. 4-[(4-Bromo-3,5-dimethylpyrazol-1-ylmethyl)]benzonitrile (2.082 g, 8.57 mmol) and 85% H_2SO_4 (20 ml) were added to a round bottom flask. The mixture was heated to 80 °C and stirred for 4 h. On completion of the stir, the solution was poured slowly over ice and the resulting brown solution was adjusted to basic pH using 5 M NaOH. The aqueous solution was washed with ethyl acetate and the organic extracts were separated, dried over $MgSO_4$ and reduced to a white solid (1.485 g, 69%). Colourless prisms suitable for X-ray diffraction were obtained from slow evaporation of acetonitrile. Mp 195–198 °C. ^{1}H NMR (δ_H; 200 MHz, $CDCl_3$): 2.149 (s, 3H), 2.246 (s, 3H), 5.284 (s, 2H), 5.835 (s, 1H), 5.984 (s, 1H), 7.125–7.165 (d, J = 8 Hz, 2H), 7.744–7.786 (d, J = 8 Hz, 2H); ^{13}C NMR (δ_C; 50 MHz, DMSO): 9.953, 12.047, 52.544, 93.283, 126.800, 127.862, 133.567, 137.284, 140.281, 144.908, 167.584; IR (KBr): 3339.40, 3185.78, 1669.99, 1623.90, 1388.34, 1070.84, 717.50, 691.89, 645.80. MS: m/z 307.969, 309.968.

3-[(Pyrazol-1-ylmethyl)]benzonitrile, 4. To a round bottom flask, Pyrazole (1.5 g, 22.1 mmol) and THF (80 ml) were added. To this solution, NaOH pellets (8.82 g, 221 mmol) were added and the reaction was stirred at room temperature for 2 h. On completion, α-bromo-*m*-tolunitrile (4.32 g, 22.1 mmol) in THF (80 ml) was added and the reaction mixture stirred at room temperature overnight. On completion, water was added to dissolve any excess NaOH, the organic layer separated off, dried over $MgSO_4$ and the solvent removed under vacuum to yield a yellow oil (3.419 g, 84.7%). ^{1}H NMR (δ_H; 400 MHz, $CDCl_3$): 5.203 (s, 2H), 6.174–6.184 (t, J = 2 Hz, 1H), 7.255 (s, 1H), 7.275–7.282 (d, J = 2.8 Hz 2H), 7.359–7.370 (t, J = 2 Hz 1H), 7.379–7.384 (d, J = 2 Hz, 1H), 7.427–7.432 (d, J = 2 Hz, 1H); IR (KBr): 3119.20, 2929.73, 2230.73, 1582.93, 1511.24, 1434.42, 1395.30, 1291.04, 1089.01, 1055.48, 973.54, 685.16.

3-[(Pyrazol-1-ylmethyl)]benzamide, 10. To a round bottom flask, 3-[(pyrazol-1-ylmethyl)]benzonitrile (2.578 g, 14.08 mmol) and 85% H_2SO_4 (10 ml) were added. The mixture was heated to 80 °C and stirred for 4 h. On completion of the stir, the solution was poured slowly over ice and the resulting brown solution was adjusted to basic pH using 5 M NaOH. The aqueous solution was washed with $CHCl_3$ and the organic extracts were separated, dried over $MgSO_4$ and reduced to a pale yellow solid (1.244 g, 44%). Colourless blocks suitable for X-ray diffraction were obtained *via* slow evaporation of ethanol. Mp 117–120 °C. ^{1}H NMR (δ_H; 400 MHz, $CDCl_3$): 5.378 (s, 2H), 5.805 (s, 1H), 6.143 (s, 1H), 6.311–6.321 (t, J = 2 Hz, 1H), 7.351–7.370 (d, J = 7.6 Hz, 1H), 7.407–7.427 (d, J = 8 Hz, 1H), 7.440 (s, 1H), 7.574 (s, 1H), 7.703 (s, 1H), 7.728–7.747 (d, J = 7.6, 1H). ^{13}C NMR (δ_C; 50 MHz, $CDCl_3$): 55.634, 106.517, 126.886, 127.182, 129.367, 129.792, 131.286, 134.147, 137.462, 139.965, 169.143; IR (KBr): 3327.03, 3149.29, 1684.49, 1388.47, 1046.25, 768.73, 761.94. MS: m/z 201.983.

3-[(3,5-Dimethylpyrazol-1-ylmethyl)]benzonitrile, 5. To a round bottom flask, 3,5-dimethylpyrazole (5 g, 52 mmol) and THF (125 ml) were added. To this solution, NaOH pellets (21 g, 520 mmol) were added and the reaction was stirred at room temperature for 2 h. On completion, α-bromo-*m*-tolunitrile (10.4 g, 52 mmol) in THF (125 ml) was added and the reaction mixture stirred at room temperature for 3 days. On completion, water was added to dissolve any excess NaOH, the organic layer was separated off, dried over $MgSO_4$ and the solvent removed under vacuum to yield a white solid (10.58 g, 96.3%). Mp 33–35 °C. ^{1}H NMR (δ_H; 400 MHz, $CDCl_3$): 2.165 (s, 3H), 2.247 (s, 3H), 5.242 (s, 2H), 5.896 (s, 1H), 7.301–7.39 (d, J = 7.6 Hz, 2H), 7.391–7.466 (t, J = 7.6, 1H), 7.524–7.561 (d, J = 7.4, 1H); IR (KBr): 3111.60, 2939.23, 2223.20, 1619.89, 1500.55, 1447.51, 1387.85, 1275.14, 1076.24, 1036.46, 950.28, 824.31, 744.75.

3-[(3,5-Dimethylpyrazol-1-ylmethyl)]benzamide, 11. 3-[(3,5-Dimethylpyrazol-1-ylmethyl)]benzonitrile (0.3 g, 1.42 mmol) and 85% H_2SO_4 (3 ml) were added to a round bottom flask. The mixture was heated to 80 °C and stirred for 4 h. On completion of the stir, the solution was poured slowly over ice and the resulting brown solution was adjusted to basic pH using 5 M NaOH. The aqueous solution was washed with $CHCl_3$ and the organic extracts were separated, dried over $MgSO_4$ and reduced to a white solid (0.203 g, 62.4%). Colourless plates suitable for X-ray diffraction were obtained *via* slow evaporation of ethanol. Mp 158–161 °C. ^{1}H NMR (δ_H; 400 MHz, $CDCl_3$): 2.158 (s, 3H), 2.247 (s, 3H), 5.245 (s, 2H), 5.867 (s, 1H), 5.963 (s, 1H), 6.219 (s, 1H), 7.189–7.209 (d, J = 8 Hz, 1H), 7.362–7.401 (t, J = 7.6 Hz, 1H), 7.574 (s, 1H), 7.684–7.703 (d, J = 7.6 Hz, 1H); ^{13}C NMR (δ_C; 50 MHz, $CDCl_3$): 11.167, 13.542, 52.180, 105.839, 125.715, 126.550, 129.129, 130.260, 133.863, 138.119, 139.288, 147.982, 168.996; IR (KBr): 3354.77, 3288.19, 3139.69, 2919.49, 1680.23, 1603.41, 1547.08, 1454.91, 1372.97, 784.07, 707.25. MS: m/z 230.033.

3-[(4-Bromo-3,5-dimethylpyrazol-1-ylmethyl)]benzonitrile, 6. To a round bottom flask, 4-bromo-3,5-dimethylpyrazole (1.5 g, 8.57 mmol) and THF (25 ml) were added. To this solution, NaOH pellets (3.43 g, 85.7 mmol) were added and the reaction was stirred at room temperature for 2 h. On completion, α-bromo-*m*-tolunitrile (1.68 g, 8.57 mmol) in THF (25 ml) was added and the reaction mixture stirred at room temperature for 2 days. On completion, water was added to dissolve any excess NaOH, the organic layer was separated off, dried over $MgSO_4$ and the solvent removed under vacuum to yield a white solid (2.25 g, 90.5%). Mp 72–75 °C. ^{1}H NMR (δ_H; 200 MHz, $CDCl_3$): 2.174 (s, 3H), 2.222 (s, 3H), 5.270 (s, 2H), 7.328–7.367 (d, J = 7.8 Hz, 2H), 7.400–7.473 (t, J = 7.4 Hz, 1H), 7.528–7.567 (d, J = 7.8 Hz, 1H); IR (KBr): 3027.03,

2924.61, 2228.17, 1541.96, 1470.27, 1265.43, 1070.43, 906.97, 804.55, 702.13.

3-[(4-Bromo-3,5-dimethylpyrazol-1-ylmethyl)]benzamide, 12. To a round bottom flask, 3-[(4-bromo-3,5-dimethylpyrazol-1-ylmethyl)]benzonitrile (0.3 g, 1.03 mmol) and 85% H_2SO_4 (3 ml) were added. The mixture was heated to 80 °C and stirred for 4 h. On completion, the solution was poured slowly over ice and the resulting brown solution was adjusted to basic pH using 5 M NaOH. The aqueous solution was washed with chloroform and the organic extracts were separated, dried over $MgSO_4$ and reduced to a white solid (0.125 g, 39%). Colourless plates suitable for X-ray diffraction were obtained from the co-crystallisation reaction with fumaric acid *via* slow evaporation of acetonitrile. Mp 133–136 °C. ^{1}H NMR (δ_H; 200 MHz, $CDCl_3$): 2.150 (s, 3H), 2.220 (s, 3H), 5.240 (s, 2H), 6.513 (s, 2H), 7.169–7.208 (d, J = 7.8 Hz, 1H), 7.283–7.400 (m, J = 8 Hz, 1H), 7.644 (s, 1H), 7.678–7.717 (d, J = 7.8 Hz, 1H); ^{13}C NMR (δ_C; 50 MHz, $CDCl_3$): 10.560, 12.464, 53.553, 94.937, 126.163, 126.906, 129.304, 130.404, 134.227, 137.360, 137.580, 146.654, 169.474; IR (KBr): 3354.77, 3165.29, 2919.49, 1659.74, 1408.82, 1296.16, 1065.72, 804.55, 737.98, 661.17. MS: m/z 307.985, 309.985.

X-Ray crystallography

Datasets were collected on a Bruker diffractometer at the indicated temperature using Mo-Kα radiation, Table 1.

CCDC reference numbers 653212–653217.

For crystallographic data in CIF or other electronic format see DOI: 10.1039/b715610c

Data were collected using SMART[15] or APEXII software.[16] Initial cell constants were found by small widely separated "matrix" runs. An entire hemisphere of reciprocal space was collected. Scan speed and scan width were chosen based on scattering power and peak rocking curves. Unit cell constants and orientation matrix were improved by least-squares refinement of reflections thresholded from the entire dataset. Integration was performed with SAINT,[17] using this improved unit cell as a starting point. Precise unit cell constants were calculated in SAINT from the final merged dataset. Lorenz and polarization corrections were applied. Except where noted, absorption corrections were not applied. Data were reduced with SHELXTL.[18] The structures were solved in all cases by direct methods without incident. Where possible, the coordinates of the amide hydrogens were refined. All other hydrogens were assigned to idealized positions and were allowed to ride. All molecules were fully ordered and no solvent was present in any of the samples. Coordinates for the amide hydrogen atoms H17A, H17B in **7** were allowed to refine. Coordinates for the amide hydrogen atoms H17A, H17B in **8** were allowed to refine. Coordinates for the amide hydrogen atoms H27A, H27B in **9** were allowed to refine. Atoms C15 and C17 were unstable to anisotropic refinement and were given isotropic thermal parameters. Coordinates for the amide hydrogen atoms H27A, H27B in **10** were allowed to refine. Data were corrected for absorption. Coordinates for the amide hydrogen atoms H17A, H17B in **11** were allowed to refine. Compound **12** crystallized with two independent molecules per asymmetric unit. Data were corrected for absorption. Amide hydrogen atoms H27A, H27B and H47A, H47B were placed in idealized positions and were allowed to ride.

Results

In order to rank the hydrogen-bonding capability of the N-heterocyclic compounds included in this study, we also calculated molecular electrostatic potential (MEP) surfaces for the relevant compounds,[19] Table 2. It has previously been shown[20] that such an approach is feasible even if the

Table 1 Crystallographic data for **7–12**

	7	**8**	**9**	**10**	**11**	**12**
Formula moiety	$C_{11}H_{11}N_3O$	$C_{13}H_{15}N_3O$	$C_{13}H_{14}N_3OBr$	$C_{11}H_{11}N_3O$	$C_{13}H_{15}N_3O$	$C_{13}H_{14}N_3OBr$
Empirical formula	$C_{11}H_{11}N_3O$	$C_{13}H_{15}N_3O$	$C_{13}H_{14}N_3OBr$	$C_{11}H_{11}N_3O$	$C_{13}H_{15}N_3O$	$C_{13}H_{14}N_3OBr$
M_r	201.23	229.28	308.18	201.23	229.28	308.18
Crystal system	Monoclinic	Monoclinic	Monoclinic	Triclinic	Triclinic	Triclinic
Space group, Z	$P2_1/c$, 4	$P2_1/n$, 4	$P2_1/n$, 4	$P\bar{1}$, 2	$P\bar{1}$, 2	$P\bar{1}$, 4
a/Å	21.660(4)	8.4005(7)	12.437(3)	7.7873(5)	8.0162(4)	8.9062(12)
b/Å	4.7544(9)	8.0671(7)	8.8195(17)	8.1130(6)	8.0603(4)	11.6933(18)
c/Å	9.9321(19)	18.0477(18)	12.468(2)	8.8400(6)	10.4542(5)	14.146(2)
α/°	90.00	90.00	90.00	77.6610(10)	97.253(2)	73.396(9)
β/°	93.912(3)	102.621(6)	114.488(6)	74.4600(10)	106.060(2)	74.274(9)
γ/°	90.00	90.00	90.00	68.3980(10)	109.335(2)	70.553(9)
V/Å^3	1020.4(3)	1193.50(19)	1244.7(4)	496.14(6)	594.57(5)	1305.8(3)
T/K	100(2)	173(2)	100(2)	100(2)	100(2)	173(2)
D_c/g cm^{-3}	1.310	1.276	1.645	1.347	1.281	1.568
λ(Mo-Kα)/Å	0.71073	0.71073	0.71073	0.71073	0.71073	0.71073
μ/mm^{-1}	0.088	0.084	3.294	0.091	0.084	3.140
Θ_{min}/°	1.88	2.31	2.93	2.41	2.09	1.53
Θ_{max}/°	28.40	28.26	33.14	30.00	31.00	27.33
Reflections:						
Collected	7149	8390	58663	5729	21375	15893
Independent	2429	2789	4624	2838	3757	5718
Observed	1474	1646	3856	2546	3010	2902
Threshold expression	$>2\sigma(I)$	$>2\sigma(I)$	$>2\sigma(I)$	$>2\sigma(I)$	$>2\sigma(I)$	$>2\sigma(I)$
R_1 (observed)	0.0522	0.0491	0.0234	0.0449	0.0434	0.0704
wR_2 (all)	0.1342	0.1309	0.0622	0.1292	0.1299	0.2376

Table 2 Molecular electrostatic surface potential calculations

Ligand	E(N)/kJ mol^{-1}	Ligand	$E(N_{Pz})^a$/kJ mol^{-1}
Isonicotinamide	−247	**7**	−236.3
Nicotinamide	−255	**8**	−246.2
Pyrazine	−237, −178	**9**	−228.9
3-[Benzimidazol-1-yl)methyl]benzamide	−285	**10**	−254.5
3-[(2-Chlorobenzimidazol-1-yl)methyl]benzamide	−277	**11**	−262.2
4-[(2-Methylbenzimidazol-1-yl)methyl]benzamide	−303	**12**	−239.0

[a] $E(N_{Pz})$ represents the calculated electrostatic potential on the aromatic unsubstituted nitrogen atom.

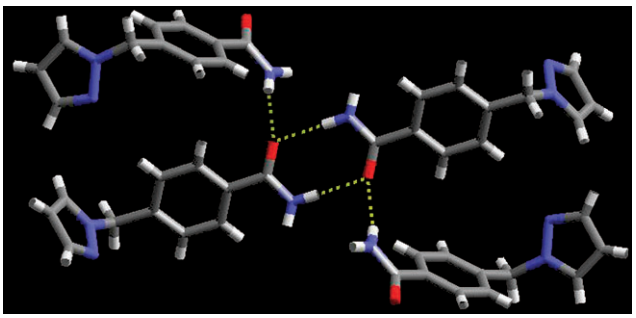

Fig. 1 The dominating intermolecular hydrogen bonds in the crystal structure of **7**.

calculations are performed at a relatively low level of theory (AM1), which makes this a versatile and readily accessible tool.

The primary intermolecular motif in the crystal structure of **7** is an amide–amide dimer constructed from two symmetry related N–H···O hydrogen bonds (2.899(2) Å). These dimers are subsequently linked into an infinite 1-D chain *via* secondary N–H···O interactions (2.938(2) Å) between the *anti* amide hydrogen atom and the carbonyl oxygen of an adjacent amide, Fig. 1.

Although a 'classic' ladder is not formed, the same hydrogen-bond interactions are present in the structure of **7**, as those that combine to form a ladder motif. The potentially competing hydrogen-bond acceptor, the pyrazole moiety, does not participate in any strong hydrogen bonds.

The crystal structure of **8** again shows the formation of the symmetry related homomeric amide···amide dimer *via* N–H···O hydrogen bonds (2.913(2) Å), Fig. 2. The network is extended *via* secondary N–H···N interactions (3.112(2) Å) between the *anti* amide hydrogen atom and the pyrazole

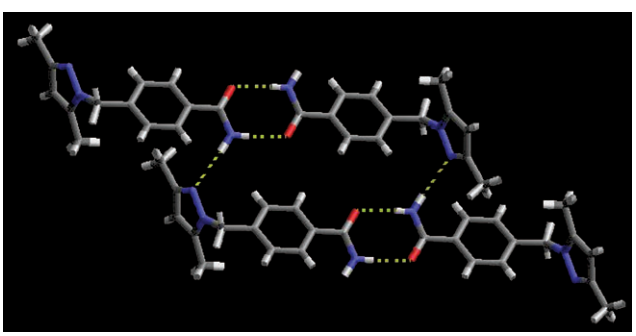

Fig. 2 Crystal structure of **8** showing dimers (constructed from an amide···amide synthon), interconnected *via* N–H···N interactions.

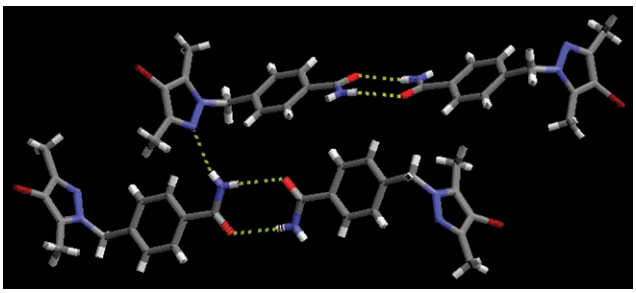

Fig. 3 Crystal structure of **9** showing homomeric dimer with hydrogen bonding to the pyrazole.

nitrogen of an adjacent ligand which demonstrates how the ladder can be disrupted by a suitably competitive acceptor.

The crystal structure of **9** shows that homomeric dimer between two amide moieties *via* N–H···O hydrogen bonds (2.9488(15) Å), Fig. 3 are present. Again, the *anti* hydrogen atom of the amide forms a N–H···N hydrogen bond (3.0341(15) Å) to an adjacent pyrazole moiety. The bromo substituent on the pyrazole is not participating in any specific or directional non-covalent interactions.

The N–H···O hydrogen bond (2.9183(11) Å) is again observed in compound **10** resulting in the formation of the homomeric amide synthon, Fig. 4. Dimers interact *via* secondary N–H···N interactions (3.0580(12) Å) between the *anti* amide hydrogen atom and an adjacent pyrazole site. The result is a 1 : 1 cyclic motif which, combined with the amide···amide dimer, leads to an extended 1-D motif.

The crystal structure of **11** shows the same type of arrangement observed in **10** with the formation of the self-complementary amide···amide dimer *via* N–H···O hydrogen bonds

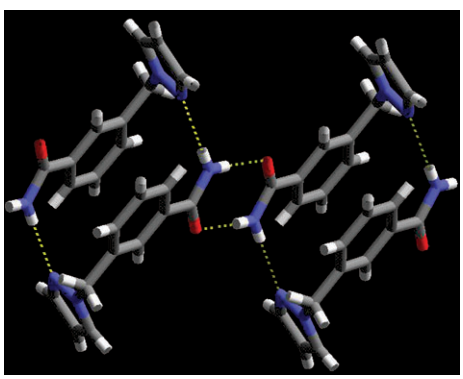

Fig. 4 Crystal structure of **10** showing dimers (constructed from amide···amide synthons), interconnected *via* N–H···N interactions.

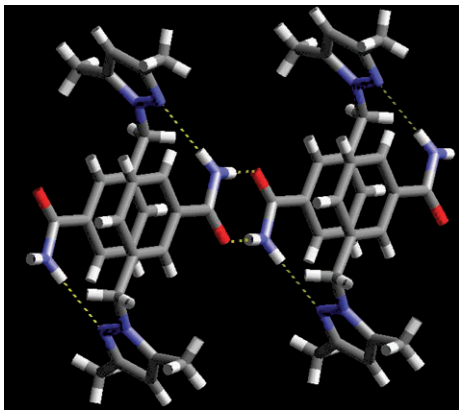

Fig. 5 Crystal structure of **11** showing amide···amide generated dimers bridged by N–H···N interactions.

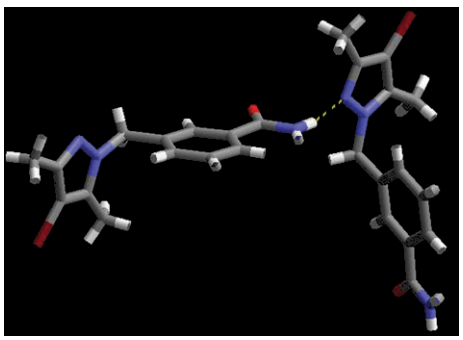

Fig. 6 Crystal structure of **12** showing a 1-D chain *via* N–H···N hydrogen bonds.

(2.9033(12) Å), Fig. 5. The network is extended into the cyclic type arrangement *via* secondary N–H···N interactions (2.9997(12) Å) between the *anti* amide hydrogen atom and the pyrazole nitrogen of an adjacent ligand.

The crystal structure of **12** is quite different from the other compounds in this study demonstrating how simple changes in molecular conformation and structure can play a major role in determining the overall arrangement in the solid-state structure. The primary motif in **12**, is a 1-D chain resulting from N–H···N hydrogen bonds between the *syn* amide hydrogen atom and the pyrazole nitrogen, Fig. 6. Each ligand possesses two different N–H···N interactions with distances of 2.709(7) and (2.671(6) Å, respectively. The carbonyl moiety and the *anti* hydrogen atom of the amide functionality both interact with aromatic C–H groups and, as was the case in **9**, the bromo substituent on the pyrazole is not participating in any specific non-covalent interaction.

Discussion

Although the new structures presented here offer some insight into the structural consequences of having the amide moiety presented with potentially disruptive hydrogen-bond moieties, it was necessary to complement our data with existing crystallographic information from the CSD[13] in order to identify structural patterns and trends. All compounds included in this search are listed in Tables 3 and 4, accompanied by their graph-set notation.[21]

Table 3 Graph set notations for substituted benzamides (CSD codes in bold in parentheses)

Ligand	N1	N2	N3	N4
2-F Bzamide **(BIGSUF)**	$2C_1^1(4)$ 2D	$4C_2^2(4)$	$4C_3^2(7)$	$R_4^2(8)$
2-Cl Bzamide #1[a] **(CLBZAM10)**	$C_1^1(4)$ $R_2^2(8)$	$R_4^2(8)$	N/A	N/A
2-Cl Bzamide #2[a] **(CLBZAM11)**	$2C_1^1(4)$	$C_2^2(8)$	N/A	N/A
2-I Bzamide **(IBNZAM)**	$C_1^1(4)$ $R_2^2(8)$	$R_4^2(8)$	N/A	N/A
3-F Bzamide **(BENAFM10)**	$C_1^1(4)$ $R_2^2(8)$	$R_4^2(8)$	N/A	N/A
3-Br Bzamide **(BRBZAM)**	$C_1^1(4)$	N/A	N/A	N/A
3-I Bzamide **(DUMNUU)**	$C_1^1(4)$ $R_2^2(8)$	$R_4^2(8)$	N/A	N/A
4-F Bzamide **(BENAFP01)**	$C_1^1(4)$ $R_2^2(8)$	$R_4^2(8)$	N/A	N/A
4-Br Bzamide #1[a] **(BBEZAM)**	$C_1^1(4)$ $R_2^2(8)$	$R_4^2(8)$	N/A	N/A
4-Br Bzamide #2[a] **(BBEZAM01)**	$C_1^1(4)$ $R_2^2(8)$	$R_4^2(8)$	N/A	N/A
4-I Bzamide **(IOBZAM)**	$C_1^1(4)$ $R_2^2(8)$	$R_4^2(8)$	N/A	N/A
2-NO_2 Bzamide **(ONBZAM)**	$C_1^1(4)$ $R_2^2(8)$	$R_4^2(8)$	N/A	N/A
3-NO_2 Bzamide **(JACYOB)**	$C_1^1(4)$ $R_2^2(8)$	$C_3^2(8)$	N/A	N/A
4-NO_2 Bzamide #1[a] **(NTBZAM01)**	$C_1^1(4)$ $R_2^2(8)$	$C_4^4(18)$	N/A	N/A
4-NO_2 Bzamide #2[a] **(NTBZAM11)**	$C_1^1(4)$ $2C_1^1(9)$	$R_1^2(4)$ $2R_4^4(24)$	$C_3^3(22)$	N/A
3-CN Bzamide **(WUKHUF)**	$R_2^2(8)$ $R_2^2(16)$	$C_4^4(20)$	N/A	N/A
2-MeO Bzamide **(RECQIA)**	$2C_1^1(4)$	$C_2^2(8)$	N/A	N/A

[a] #1 and #2 indicate different polymorphs.

Ten of the seventeen benzamides (59%) decorated with a weak hydrogen-bond acceptor (such as a halogen, nitro, cyano or methoxy substituent), contain the 'classic' $R_2^2(8)$ $R_4^2(8)$ ladder. It seems that moieties belonging to this group of relatively weak hydrogen-bond acceptors compete reasonably effectively for the *anti* hydrogen atom of the amide moiety leading to a disruption of the ladder. The amide···amide dimer, on the other hand, is present in thirteen of the seventeen structures (76%).

However, the introduction of a more competitive hydrogen-bond acceptor, such as an N-heterocyclic moiety does create major disruptions to amide···amide interactions, Table 4.

When an N-heterocyclic compound (or an N-oxide thereof) is present on the same molecular backbone as the amide itself, the ladder does not survive in any of the eighteen cases examined in this study. Instead, in eleven of eighteen structures, neighboring amide···amide dimers are connected into a chain-like motif and in the remaining seven cases, not even the amide···amide dimer survives.

We are now in a position to provide answers to the questions posed at the beginning of this study. The ladder is shown to persist in 10 of the 35 structures (29%) examined herein, whereas the amide···amide dimer is present in 24 of the 35

Table 4 Graph set notations for N-heterocycles (CSD codes in bold in parentheses)

Ligand	N1	N2	N3	N4
Isonicotinamide #1[a] **(EHOWIH01)**	$C_1^1(4)$ $R_2^2(8)$	$C_4^3(12)$	N/A	N/A
Isonicotinamide #2[a] **(EHOWIH02)**	$2C_1^1(4)$ $2C_1^1(7)$	$2R_4^4(20)$	N/A	N/A
Nicotinamide **(NICOAM01)**	$C_1^1(4)$ $C_1^1(6)$	$R_4^4(18)$	N/A	N/A
Pyrazine carboxamide #1[a] **(PYRZIN02)**	$R_2^2(8)$	N/A	N/A	N/A
Pyrazine carboxamide #2[a] **(PYRZIN01)**	$C_1^1(4)$ $R_2^2(8)$	$C_4^3(12)$	N/A	N/A
Pyrazine carboxamide #3[a] **(PYRZIN15)**	$R_2^2(8)$ $R_2^2(10)$	$C_4^4(14)$	N/A	N/A
Isonicotinamide *N*-oxide **(MEGDAE)**	$2C_1^1(8)$	$C_4^4(32)$	N/A	N/A
Nicotinamide *N*-oxide **(MEGDEI)**	$C_1^1(7)$ $R_2^2(14)$	$C_4^3(18)$	N/A	N/A
Pyrazine carboxamide *N*-oxide **(MEGDUY)**	3D	$2R_8^4(8)$ $R_4^4(28)$	$C_5^4(32)$	N/A
3-[Benzimidazol-1-yl)methyl]benzamide **(WANBUJ)**	4D	$2C_4^4(24)$ $2C_4^4(28)$ $R_2^2(8)$ $R_2^2(20)$	$2C_4^3(18)$	$R_4^4(26)$
3-[(2-Chlorobenzimidazol-1-yl)methyl]benzamide **(WANCEU)**	4D	$2C_4^4(24)$ $2C_4^4(28)$ $R_2^2(8)$ $R_2^2(20)$	$2C_4^3(18)$	$R_4^4(26)$
4-[(2-Methylbenzimidazol-1-yl)methyl]benzamide **(WANCAQ)**	$C_1^1(4)$	$C_1^1(11)$	N/A	$C_4^4(26)$
7	$C_1^1(4)$ $R_2^2(8)$	$C_4^3(12)$	N/A	N/A
8	$C_1^1(10)$ $R_2^2(8)$	$R_4^4(24)$	N/A	N/A
9	$C_1^1(10)$ $R_2^2(8)$	$R_4^4(24)$	N/A	N/A
10	$R_2^2(8)$ $R_2^2(18)$	$C_4^4(22)$	N/A	N/A
11	$R_2^2(8)$ $R_2^2(18)$	$C_4^4(22)$	N/A	N/A
12	2D	$C_4^4(36)$	N/A	N/A

[a] #1, #2 and #3 indicate different polymorphs.

structures (69%). There is a dramatic difference to the way in which weak and strong hydrogen-bond acceptors influence the outcome in structures containing an amide moiety. For weak acceptors (such as $-NO_2$, –OMe –CN, –Cl, –Br), the frequency of ladder and amide disruption is 41 and 23%, respectively.

However, with stronger hydrogen-bond acceptors (N-heterocycles and N-oxides thereof), the corresponding numbers are 100 and 39%, respectively. It is noteworthy that it is possible to provide a more detailed ranking of the hydrogen-bond accepting capability within the latter group even further. The calculated MEP values for the heterocycles included in this study, Table 2, indicate that pyrazine, pyrazole, and pyridine are expected to be less competitive than the benzimidazole/N-oxide acceptors. In fact, the dimer is broken 3/12 (25%) times for the former group, and 4/6 (67%) for the latter group. The hydrogen-bond acceptor strength as determined by calculated MEPs, which is consistent with reported pK_{HB} data,[22] is directly translated into structural consequences in these structures.

Conclusions

Although the amide···amide ladder is a well-known and readily recognizable supramolecular construction, this motif is not particularly stable (10/35) in the presence of potentially competing intermolecular interactions. On the other hand, the amide···amide dimer, which is a structural pre-requisite for ladder formation, is considerably more prevalent (24/35) in the face of a variety of competing sites.

The likelihood of breaking either ladder or dimer, can be rationalized by considering the strength of the competing hydrogen-bond moiety, which offers helpful guidelines for predicting the primary intermolecular interactions involving a range of molecules equipped with an amide moiety.

Acknowledgements

We are grateful for financial support from the Terry C. Johnson Cancer Foundation, DURIP (49806-CH-RIP) and NSF (CBET 0609318).

References

1 (*a*) L. MacGillivray, *CrystEngComm*, 2004, **6**, 77; (*b*) J.-M. Lehn, *Science*, 2002, **295**, 2400; (*c*) M. C. Etter, *J. Phys. Chem.*, 1991, **95**, 4601; (*d*) B. Moulton and M. J. Zaworotko, *Chem. Rev.*, 2001**101**, 1629; (*e*) L. Pauling, *The Nature of the Chemical Bond*, Cornell University Press, Ithaca, NY, 1939; (*f*) J.-M. Lehn, *Angew. Chem., Int. Ed. Engl.*, 1990, **29**, 1304; (*g*) J.-M. Lehn, *Supramolecular Chemistry*, VCH, Weinheim, 1995; (*h*) J. W. Steed and J. L. Atwood, *Supramolecular Chemistry*, John Wiley and Sons Ltd, Chichester, 2000.

2 (*a*) S. Kim, K. Takeda and S. Sasatani, *Eur. Pat. Appl.*, 1988; (*b*) B. T. Flatt, X. H. Gu, R. Martin, R. Mohan, B. Murphy, M. C. Nyman, W. C. Stevens, T. L. Wang and L. C. Bannen, *PCT Int. Appl.*, 2007.

3 D. A. P. Delnoye, R. P. Sijbesma, J. A. J. M. Vekemans and E. W. Meijer, *J. Am. Chem. Soc.*, 1996, **118**, 8717.

4 R. Kleppinger, C. P. Lillya and C. J. Yang, *J. Am. Chem. Soc.*, 1997, **119**, 4097.

5 (*a*) H. Yu, H. Mizufune, K. Uenaka, T. Moritoki, K. Tatsuya and H. Koshima, *Tetrahedron*, 2005, **61**, 8932; (*b*) M. George, S. L.

Snyder, P. Terech, C. J. Glinka and R. G. Weiss, *J. Am. Chem. Soc*., 2003, **125**, 10275; (*c*) R. E. Melendez, A. J. Carr, B. R. Linton and A. D. Hamilton, *Struct. Bonding*, 2000, **96**, 31.
6 M. Cavallini, F. Biscarini, S. Leon, F. Zerbetto, G. Bottari and D. A. Leigh, *Science*, 2003, **299**, 531.
7 (*a*) J. Bernstein, *J. Phys. D: Appl. Phys*., 1993, **26**, B66; (*b*) J. Bernstein, in *Organic Solid State Chemistry*, ed. G. R. Desiraju, Elsevier, New York, 1987, vol. 32, p. 471.
8 G. R. Desiraju, *Angew. Chem., Int. Ed. Engl*., 1995, **34**, 2311.
9 (*a*) G. R. Desiraju, *Crystal Engineering The Design of Organic Solids*, Elsevier, New York, 1989, vol. 54; (*b*) G. R. Desiraju, *Acc. Chem. Res*., 2002, **35**, 565; (*c*) C. B. Aakeröy and D. J. Salmon, *CrystEngComm*, 2005, **7**, 439.
10 G. A. Jeffrey and W. Saenger, *Hydrogen Bonding in Biological Structures*, Springer-Verlag, Berlin, Heidelberg, New York, 1991.
11 (*a*) L. Leiserowitz and A. T. Hagler, *Proc. Soc. R. London, Ser. A*, 1983, **388**, 133; (*b*) S. S. Kuduva, D. Bläser, R. Boese and G. R. Desiraju, *J. Org. Chem*., 2001, **66**, 1621.
12 (*a*) M. Tonogaki, T. Kawata, S. Ohba, Y. Iwata and I. Shibuya, *Acta Crystallogr. Sect. B: Struct. Sci*., 1993, **49**, 1031; (*b*) F. di Rienzo, A. Domenicano and E. Foresti Serantoni, *Acta Crystallogr. Sect. B: Struct. Crystallogr. Cryst. Chem*., 1977, **33**, 3854; (*c*) P. G. Jones, H. Thonnessen, R. Schmutzler and A. K. Fischer, *Acta Crystallogr. Sect. E: Struct. Rep. Online*, 2002, **58**, o1436.
13 Cambridge Structural Database version 5.28 (November 2006).
14 A. Osawa, T. Kaiho, T. Ito, M. Okada, C. Kawabata, K. Yamaguchi and H. Igeta, *Chem. Pharm. Bull*., 1988, **36**, 3638.
15 SMART v5.060, © 1997–1999, Bruker Analytical X-ray Systems, Madison, WI.
16 APEXII v1.27, © 2005, Bruker Analytical X-ray Systems, Madison, WI.
17 SAINT v6.02, © 1997–1999, Bruker Analytical X-ray Systems, Madison, WI.
18 SHELXTL v5.10, © 1997, Bruker Analytical X-ray Systems, Madison, WI.
19 Molecular structures for **7–12** were constructed using Spartan '04 (Wavefunction, Inc. Irvine, CA). All six molecules were optimized using AM1, with the maxima and minima in the electrostatic potential surface (0.002 e au^{-1} isosurface) determined using a positive point charge in the vacuum as a probe.
20 C. A. Hunter, *Angew. Chem., Int. Ed*., 2004, **43**, 5310–5324.
21 (*a*) J. Bernstein, R. E. Davis, L. Shimoni and N.-L. Chang, *Angew. Chem., Int. Ed. Engl*., 1995, **34**, 1555; (*b*) M. C. Etter, J. C. MacDonald and J. Bernstein, *Acta Crystallogr., Sect. B*, 1990, **46**, 256; (*c*) M. C. Etter, *Acc. Chem. Res*., 1990, **23**, 120.
22 C. Laurence and M. Berthelot, *Perspect. Drug Discovery Des*., 2000, **18**, 39–60.